JOURNAL OF MATERIALS SCIENCE 29 (1994) 6091–6096

The impact behaviour of paints

N. N. DIOH, J. G. WILLIAMS
Imperial College of Science, Technology and Medicine, Department of Mechanical Engineering, Exhibition Road, London SW7 2BX, UK

The split Hopkinson pressure bar has been used to study the impact behaviour of a selection of single and multi-layer paint systems in the form of films of thickness 0.04 mm. Stress–strain curves are presented for systems comprising three coatings, coating A, coating B and coating C, in compression for strain rates of the order 5×10^3 s^{-1}. A comparison is made between the high strain-rate behaviour and that seen at quasi-static strain rates. All tests were carried out at 23 °C. The coatings studied are shown to be strain-rate sensitive, exhibiting almost a two-fold increase in flow/yield stress between the two strain-rate regimes. At low strain rates, all the coatings deformed uniformly with no sign of fracture. At high strain rates, both coating A and coating C underwent catastrophic failure which is indicative of their susceptibility to chipping. However, this was not the case with coating B which shows no signs of fracture at high strain rates for strains up to 45 %. However, a combination of coating A and coating B in alternate layers led to catastrophic fracture of the resulting two-coat multi-layer system at high strain rates.

1. Introduction

The resistance of paints to chipping is of great importance in the automotive industry. Apart from it being visually unattractive, it exposes the substrate to attack by hostile environments which may lead to corrosion and destruction of the substrate. In addition, failure of the substrate may also take place by surface embrittlement if the substrate is painted with a thin layer of a brittle coating. While such a layer of a few microns thickness contributes nothing to the strength of the substrate, its impact resistance may be drastically reduced by an unsuitable coating [1, 2]. This is certainly of great concern when plastic substrates are used. Developing a coating which has all the necessary good qualities, i.e. weatherability, sandability, polishability, chemical resistance and impact resistance, is indeed very difficult. In order to achieve this, multi-layer combinations of various coatings are generally used. Such multiple layer systems are composed of electrocoats, primers and topcoat layers. Clearly, in such systems, it is important to determine qualitatively and quantitatively the behaviour of each single coating, the multi-layer system, and the multi-layer and substrate composite, in order to assess the overall behaviour of the component.

The quantitative characterization of paints under impact conditions is difficult and, as such, their behaviour under impact is assessed using qualitative techniques (ASTM D2794-92). Maier and Liable [3] described punching experiments at impact speeds of 4.5 m s^{-1} at temperatures down to − 25 °C for various coatings. They were able to show qualitatively the effect of strain rate and temperature on the fracture behaviour of the systems studied. In the present work, the quantitative behaviour of coatings under impact conditions has been assessed in terms of their stress–strain behaviour. Three automobile coatings for different applications have been studied. These will be referred to as coating A, coating B and coating C. The stress–strain properties of the individual coatings have been assessed, as well as a combination of layers. In addition, the susceptibility to fracture of each system was also assessed qualitatively at low and high strain rates.

2. Experimental procedure

2.1. Materials

All the materials were supplied by Dupont in the form of thin films of thickness 0.04–0.07 mm. The specimens were machined into discs of diameter 12.7 mm and thickness 4.4 or 1.0 mm, where each one was made up by stacking the films until the required thickness was obtained. Punching of the stacked films proved impossible and, as such, an alternative method involving the machining of the stacked films between pressure pads had to be devised. The machining process is shown in Fig. 1. A steel rod (1) of diameter 12.7 mm is held in the lathe chuck; (2) is also a steel rod of the same diameter which is held in place by the spinning centre; (3) is the cutting tool. The thin sheet of paper separates the specimens. Multi-layer systems are created by stacking the individual coatings one after another. At low strain rates, the 4.4 mm thick specimens were used, whereas at high strain rates the 1.0 mm thick specimens were used. This combination of thickness for low and high strain rate tests has been shown to yield accurate results at each rate [4]. Before

0022–2461

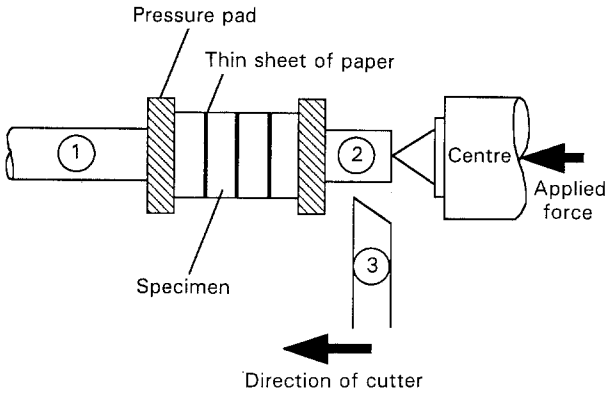

Figure 1 Specimen manufacture.

testing, each specimen was coated on its front and back faces with a thin layer of petroleum jelly, which has been shown to be an excellent lubricant for testing polymers at high strain rates [5–7].

2.2. The tests

The low-rate tests were carried out on an Instron machine. Owing to the small specimen thicknesses used, a linear voltage displacement transducer (LVDT) was used to monitor specimen deformation. Strain rate was calculated from the crosshead velocity of the machine and the initial specimen thickness.

All high-rate tests were carried out in a split Hopkinson pressure bar apparatus [8]. In its compressive configuration, this consists of two long elastic bars, an input and output, with the disc-shaped specimen sandwiched in between. Care is needed in placing the specimen between the bars to avoid the possible misalignment of the individual loose films. Both the input and output bars are made from 15.8 mm diameter high-strength aluminium (HE15). The free end of the input bar is subjected to an axial impact by a projectile made from the bar stock. This generates a compressive loading pulse which travels along the input bar towards the specimen. Owing to a difference in mechanical impedance between the bars and the specimen, interaction of the incident pulse and the specimen results in stress waves being reflected back into the input bar and also being transmitted through the specimen into the output bar. Having recorded the incident, reflected and transmitted strain pulses at fixed points in the bar (denoted by $\varepsilon_I(t)$, $\varepsilon_R(t)$ and $\varepsilon_T(t)$), the displacement conditions at the specimen–bar interfaces can be established.

The variations of stress and strain in the specimen are conventionally obtained from the following expressions [8]

$$\varepsilon_s(t) = \frac{-2C_b}{l}\int_0^t \varepsilon_R(t)\,dt \quad (1)$$

$$\sigma_s(t) = E\left(\frac{A}{A_s}\right)\varepsilon_T(t) \quad (2)$$

$$\dot{\varepsilon}_s(t) = \frac{-2C_b}{l}\varepsilon_R(t) \quad (3)$$

where $\varepsilon_s(t)$, $\sigma_s(t)$ and $\dot{\varepsilon}_s(t)$ are the variation of strain, stress and strain rate in the specimen with time. E and C_b are the Young's modulus and elastic wave speed in the bars, respectively, while l is the initial length of the specimen and A/A_s is the area ratio between the bars and the specimen. The strain pulses are shifted in time in order to be coincident at the specimen. The stress–strain relationship of the material being measured can then be obtained by eliminating time, t, between Equations 1 and 2, and the strain rate directly from Equation 3. The results of the experiments are presented below. In the present work, an impact velocity in the region of 18 m s^{-1} was employed in all the high-rate tests.

3. Results and discussion

Typical experimental results in terms of the incident, reflected and transmitted stress pulses are shown in Figs 2–4. The original stress–strain curves show a toe region which does not represent a property of the material and is an artefact associated with the take-up of slack, and alignment or seating of the specimen. This is compensated for in all the stress–strain curves shown below in accordance with the ASTM standard D695. Each stress–strain curve shown below represents the average from three tests at the same crosshead or impact velocity. The nature of the split

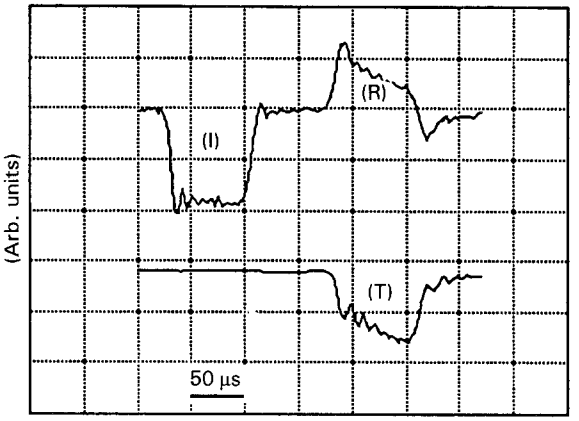

Figure 2 Typical test results for coating B at high strain rates. The letters I, R and T represent the incident, reflected and transmitted stress pulses.

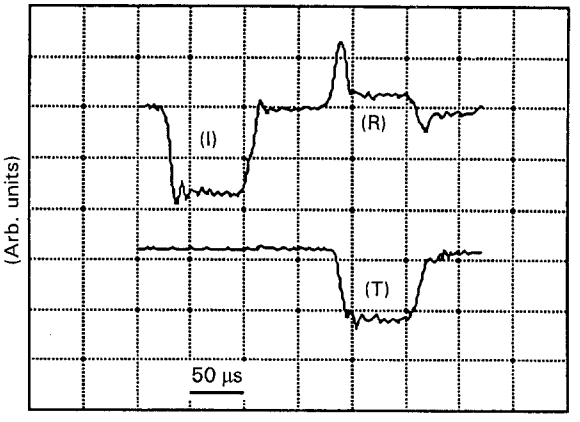

Figure 3 Typical test results for coating A at high strain rates.

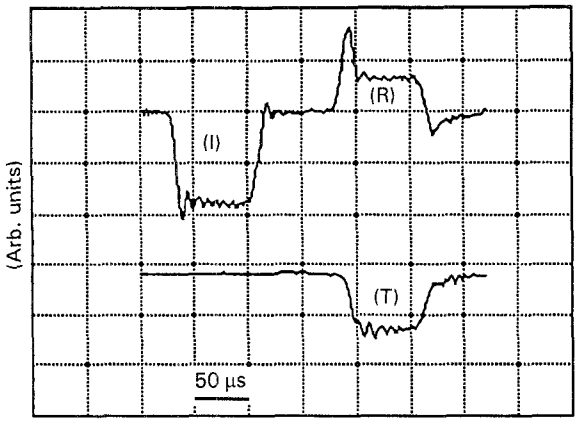

Figure 4 Typical test results for coating C at high strain rates.

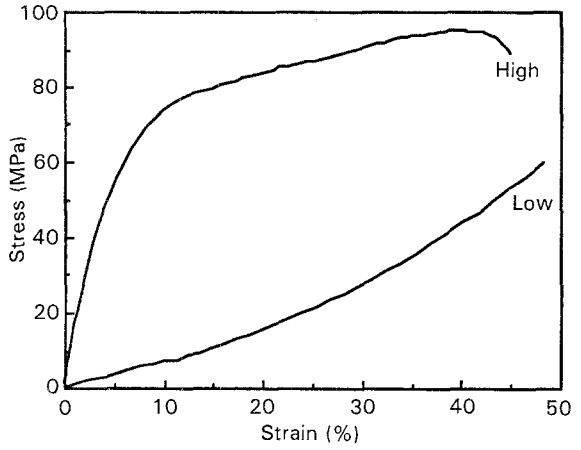

Figure 5 Stress strain curves for coating B at 23 °C at low and high strain rates. The low- and high-rate curves correspond to average strain rates of 4×10^{-3} and 3×10^{3} s^{-1}, respectively.

Hopkinson pressure bar is such that the strain rate is not constant throughout the test; as such, nominal strain rates are quoted for the high rate tests.

The difference in the impact behaviour of the coatings is immediately evident from the pulses shown in Figs 2–4. The plateaux region in the reflected and transmitted pulses seen for the primer and the EPOTUF (Figs 3 and 4) indicates a zero plastic wave speed in the material, which corresponds to subsequent zero modulus. The onset of this plateaux region signifies specimen failure.

It is clear from Fig. 5 that strain rate has a major effect on the behaviour of coating B at 23 °C. At low strain rates, it exhibits a J-type stress–strain curve, typical of biological tissues, in which its modulus increases with strain [9]. At high strain rates, its behaviour is significantly different showing a reduction in modulus with strain. This behaviour at high strain rate is characteristic of a range of polymers, such as medium- and high-density polyethylene [4]. Examination of the tested specimens shows that coating B undergoes uniform deformation at both strain-rate regimes with no sign of fracture (Fig. 6) for strains of up to 45%. This observation is encouraging because the coating B is supposed to be used in areas of the automobile which are most likely to suffer from impact damage.

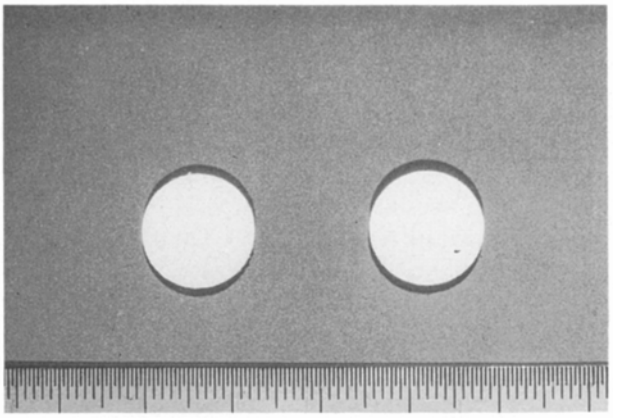

Figure 6 Photograph of tested coating B specimens at low and high strain rates. The specimen tested at high strain rates is shown on the right.

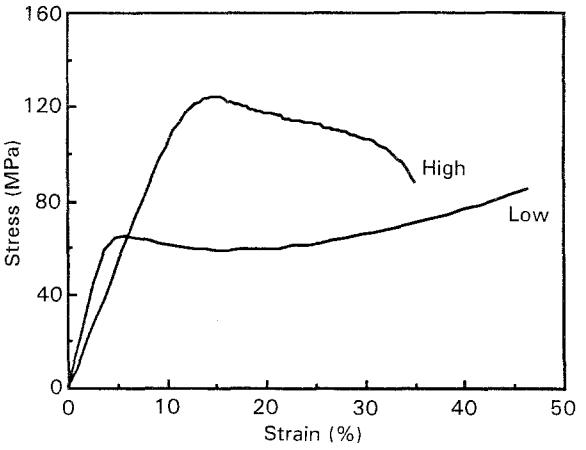

Figure 7 Stress–strain curves for coating A at 23 °C at low and high strain rates. The low- and high-rate curves correspond to average strain rates of 4×10^{-3} and 3×10^{3} s^{-1}, respectively.

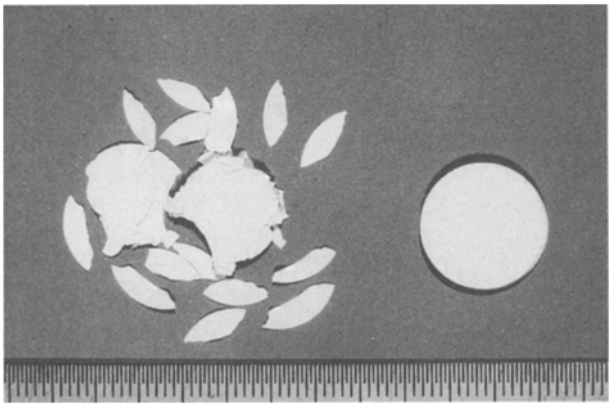

Figure 8 Photograph of tested coating A specimens at low and high strain rates. The specimen tested at high strain rates is shown on the left.

Fig. 7 shows that coating A exhibits a definite yield point in compression both at low and high rates of strain. This accounts for the plateaux region in the reflected and transmitted pulses shown in Fig. 3. There is approximately a two-fold increase in yield stress between the two strain-rate regimes. At high strain rates it shatters catastrophically, suggesting in-service chipping/fracture under impact conditions (Fig. 8). At

low strain rates, however, there is no sign of fracture for the same or even higher values of strain. The specimens corresponding to the high and low strain-rate tests are shown on the left and right of the picture. Similar results as obtained for coating A are obtained for coating C. As in the case of coating A, this material also shows a two-fold increase in yield stress between the two strain rate regimes (Fig. 9). The corresponding flow stress values, however, are lower. At high strain rates, coating C undergoes fracture whereas at low strain rates it deforms uniformly with no sign of fracture. Coating C, however, does not fail as catastrophically as coating A (Fig. 10).

In Figs 7 and 9, it can be seen that the initial Young's moduli of coating A and coating C at high strain rates appear to be slightly lower than the respective moduli at low strain rates. This, although unexpected, may be due to the presence of an air layer between the films. At low strain rates there is sufficient time for air to be squeezed out during testing. At high strain rates, however, when each test lasts for only 100 μs, there may not be enough time for the air to get squeezed out. This results in a composite structure having trapped air layers between the paint films. This is a possible explanation for why the results suggest larger fracture strains at high strain rates for these two coatings. A similar increase in fracture strain at high strain rates has also been reported for glass fibre reinforced plastics (GFRP) [10]. This was attributed to the dominance of the resin at high strain rates.

The differences in stress–strain behaviour at 23 °C between the three coatings at low and high strain rates are shown in Figs 11 and 12, respectively. It is clear from both figures that although the stress–strain behaviour of coating A is similar to that of coating C, the former yields higher flow stresses in both strain rate regimes.

Fig. 13 shows the low and high rate stress–strain curves obtained when a multi-layer specimen made up of alternate coating A and coating B films are tested. In this case, there is approximately a three-fold increase in yield stress between the two strain-rate regimes. Errors in the initial high strain-rate modulus associated with the air layer are not present because the alternate layers stick together due to the adhering nature of coating B. At low strain rates, the resulting stress–strain curve is an average of the individual curves corresponding to each coating (Fig. 14), whereas at high strain rates, the behaviour of the primer within the multi-layer specimen appears to be dominant (Fig. 15). This is also evident from Fig. 17 which

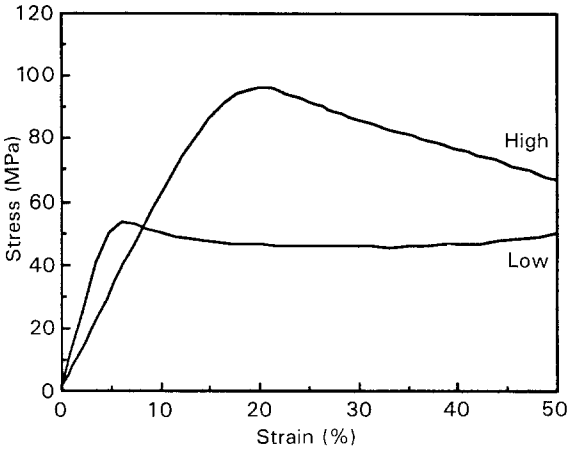

Figure 9 Stress–strain curves for coating C at 23 °C at low and high strain rates. The low- and high-rate curves correspond to average strain rates of 4×10^{-3} and 5×10^{3} s^{-1}, respectively.

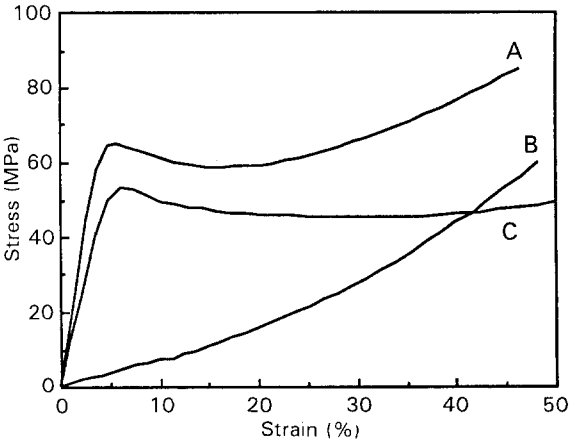

Figure 11 Stress–strain curves at 23 °C for the three coatings at low strain rates.

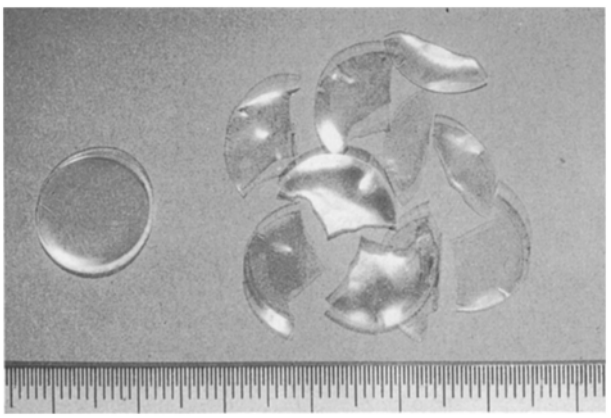

Figure 10 Photograph of tested coating C specimens at low and high strain rates. The specimen tested at high strain rates is shown on the right.

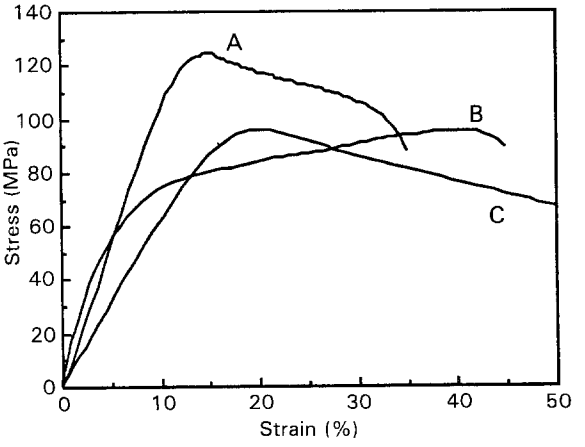

Figure 12 Stress–strain curves at 23 °C for the three coatings at high strain rates.

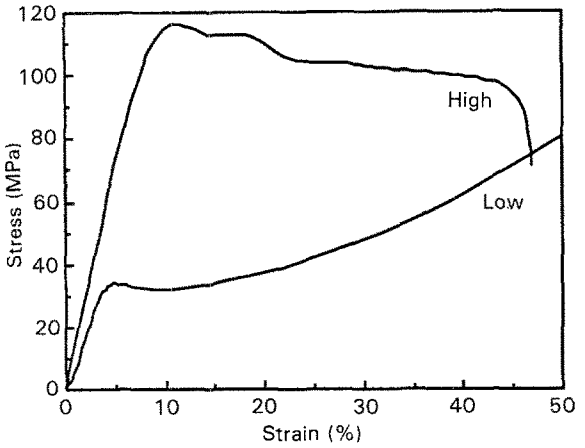

Figure 13 Stress–strain curves for coating A + coating B at 23 °C at low and high strain rates. The low- and high-rate curves correspond to average strain rates of 4×10^{-3} and 5×10^{3} s^{-1}, respectively.

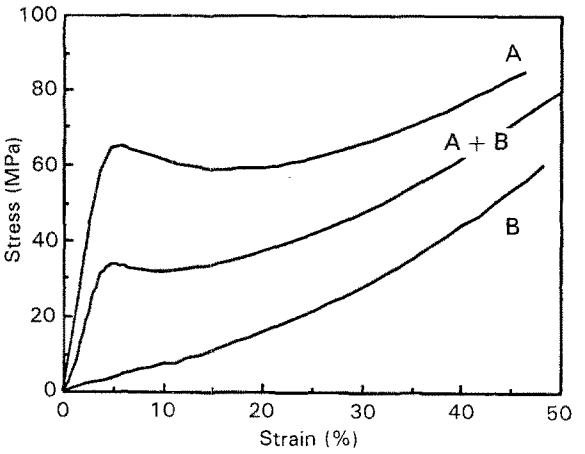

Figure 14 Stress–strain curves for coatings A, A + B and B at 23 °C at low strain rates.

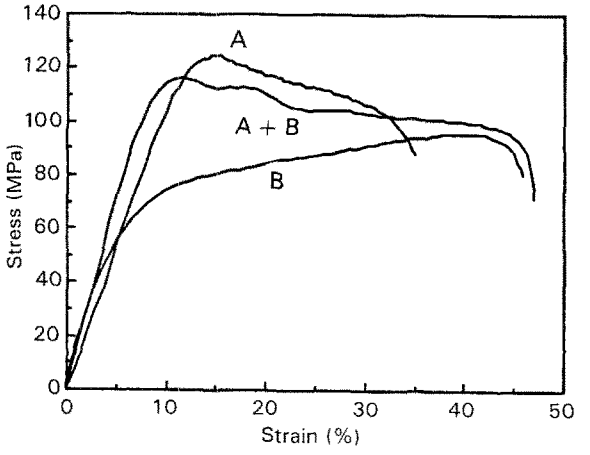

Figure 15 Stress–strain curves for coatings A, A + B and B at 23 °C at high strain rates.

shows the tested multi-layer specimen at high strain rates. The multi-layer specimen undergoes catastrophic fracture similar to that observed from tests on coating A specimens. This shows that even though coating B does not undergo fracture at high strain rates, combining it with a coating that does will result in the fracture of both layers. Embrittlement of coating B by coating A is therefore possible if both are used in the same multi-layer system. This is due to the fact that the material behaviour is now governed by the much lower dynamic fracture resistance of coating A [11].

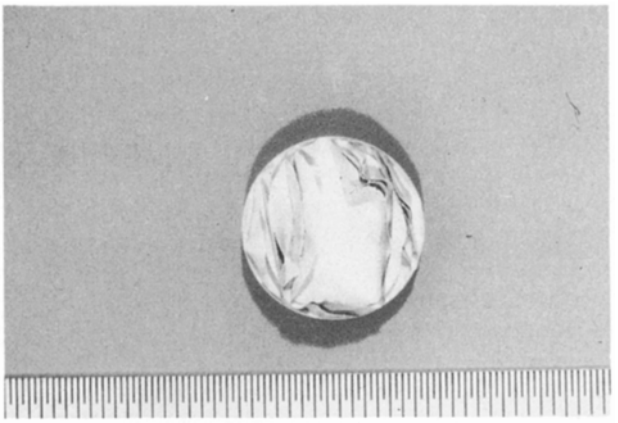

Figure 16 Photograph of tested coating (A + B) specimens at low strain rates.

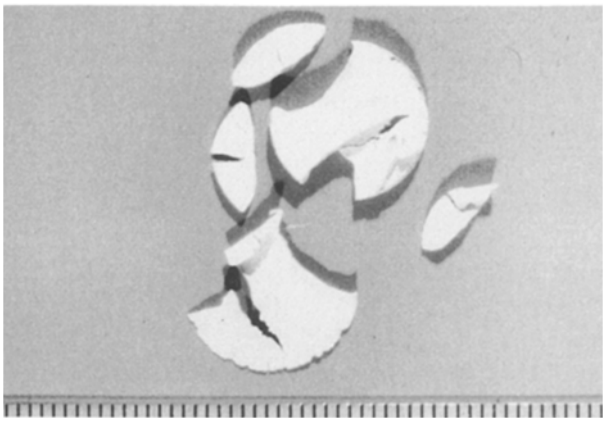

Figure 17 Photograph of tested coating (A + B) specimens at high strain rates.

The results show that the spilt Hopkinson pressure bar apparatus can be used to study the stress–strain and fracture behaviour of very thin coatings under impact conditions. Because temperatures can easily be varied in the apparatus [12], the effect of both temperature and strain rate can be studied for any given single-layer, multi-layer or multi-layer/substrate system. In this way the complete behaviour of any system can be characterized for any given strain rate and temperature range. Furthermore, using this technique, the effect of layer thickness on embrittlement can be investigated.

4. Conclusion

The effect of strain rate on the stress–strain behaviour of three automotive coatings, A, B and C, has been studied at 23 °C. At low strain rates, none of the coatings studied undergo chipping. At high strain rates, however, both coating A and coating C undergo fracture showing a two-fold increase in yield stress at high strain rates. Coating B, on the other hand, under-

goes uniform deformation with no sign of fracture. However, combining coating B with coating A to produce a multi-layer system having alternate layers of each coating results in fracture. The results show that the split Hopkinson pressure bar apparatus can be used to study the stress–strain and fracture behaviour of very thin coatings under impact conditions.

Acknowledgement

The authors thank Dr R. E. Vallerschamp, Du Pont for providing the coatings used in this work.

References

1. L. ROLLAND and L. J. BROUTMAN, *Polym. Eng. Sci.* **25** (1985) 207.
2. P. K. SO and L. J. BROUTMAN, *ibid.* **26** (1986) 1173.
3. W. MAIER and R. LIABLE, *Forsch. Entwickl.* **5** (1988) 337.
4. N. N. DIOH, P. S. LEEVERS and J. G. WILLIAMS, *Polymer* **34** (1993) 4230.
5. S. M. WALLEY, J. E. FIELD, P. H. HOPE and N. A. SAFFORD, *Phil. Trans. R. Soc. Lond.* **A328** (1989) 1.
6. S. M. WALLEY, J. E. FIELD, P. H. HOPE and N. A. SAFFORD, *J. de Phys. III Fr.* **1** (1991) 1889.
7. B. J. BRISCOE and R. W. NOSKER, *Wear* **95** (1984) 241.
8. U. S. LINDHOLM, *J. Mech. Phys. Solids* **12** (1964) 317.
9. A. G. ATKINS and Y-M. MAI, "Elastic and Plastic Fracture" (Ellis Horwood Series, Wiley, New York, 1985) p. 55.
10. J. HARDING, in "Materials at high strain rates", Edited by T. Z. Blazynski (Elsevier Applied Science, 1987) p. 133.
11. A. IVANKOVIC, PhD thesis, Department of Mechanical Engineering, Imperial College, London (1991).
12. N. N. DIOH, PhD thesis, Department of Mechanical Engineering, Imperial College, London (1993).

Received 9 February
and accepted 16 May 1994